reduced, the switching offset of the second stage must be adjusted, which can be accomplished by reducing the supply voltage. This permits reduction of the first stage transimpedance gain, thereby maintaining high bandwidth operation. Reduced supply furthermore drops the off-chip drive voltage to ~ 40mV, resulting in cleaner off-chip signalling, e.g. ~ 125mV for V_{dd} = 3.3V.

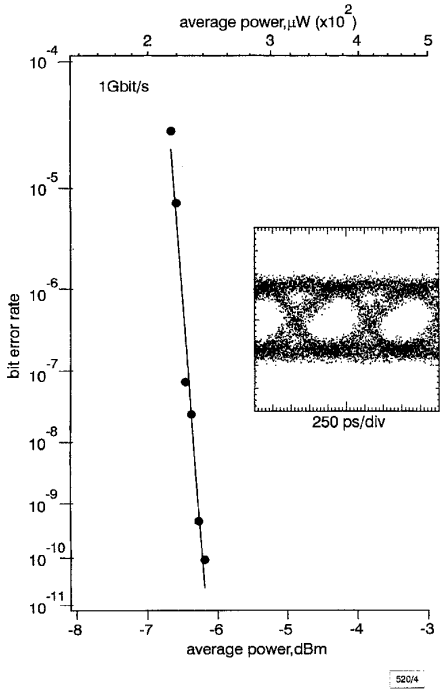

Fig. 4 *Bit error rate characteristics at 1Gbit/s and 850nm from receiver circuit*

Inset: eye diagram obtained at 10s persistence on sampling oscilloscope at BER = 10^{-9}

The off-chip signal was amplified and low-pass filtered with a 3dB cutoff frequency of 933MHz prior to taking the bit error rate (BER) and eye pattern data shown in Fig. 4. A BER of 10^{-9} is obtained at an average optical input power of –6.3dBm. The bias conditions for such operation were V_{dd} = 2.2V, V_{dd}(driver) = 3.2V, V_{tune} = –0.86V and V_{det} = 10V. Under these conditions, while operating at 1 Gbit/s, the current drawn from supply for two complete receivers including everything except the follower of Fig. 3 was 1.26mA, suggesting a single pre-amplifier dissipation of < 1.5mW. At V_{dd} = 3.3V, static dissipation increases to ~ 6mW/receiver. The minimum BER obtainable at 1.25Gbit/s was 10^{-8}. The sensitivity of the receiver improves somewhat at lower bit rates, with a BER of 10^{-9} requiring an average input power of –8.6dBm at 622Mbit/s, and –14dBm at 155Mbit/s. The relatively high input optical powers required for these measurements can be attributed to the low responsivity of the shallow *n*-well detection region. Most of the carriers collected by the *n*-well orginate in the substrate, with test diodes showing a responsivity at 850nm of ~ 0.25A/W. However, far fewer carriers are collected to the *p*-diffusion/*n*-well active diode, which exhibits a voltage dependent responsivity of ~ 0.01–0.04A/W near junction breakdown (~ 10V). While the relatively high levels of average power required to operate these receivers may appear daunting, it should be noted that in many LAN and interconnect applications, optical power is not in short supply.

In summary, we present the first operation of a fully-integrated optical receiver made entirely within a standard production CMOS process, operating to 1Gbit/s at a wavelength of 850nm. Our results bode well for the use of standard CMOS processes in many new optoelectronic applications.

Acknowledgments: We are pleased to acknowledge the technical assistance of J. Salata and D. Inglis of Lucent Technologies.

Electronics Letters Online No: 19980855 *20 March 1998*

T.K. Woodward and A.V. Krishnamoorthy (*Bell Laboratories, Lucent Technologies, Holmdel, NJ 07733-3030, USA*)

References

1 KUCHTA, D.M., AINSPAN, H.A., CANORA, F.J., and SCHEIDER, R.P., Jr.: 'Performance of fiber-optic data links using 670-nm cw VCSELS and a monolithic Si photodetector and CMOS preamplifier', *IBM J. Res. Dev.*, 1995, **30**, (12), pp. 63–72

2 KIM, H.H., SWARTZ, R.G., OTA, Y., WOODWARD, T.K., FEUER, M.D., and WILSON, W.L.: 'Prospects for silicon monolithic opto-electronics with polymer light-emitting diodes', *J. Lightwave Technol.*, 1994, **12**, (12), pp. 2114–2121

3 LALANNE, P., and RODIER, J.-C.: 'CMOS photodiodes based on vertical p-n-p junctions'. Workshop on Optics and Computer Science, Proc. 11th Int. Parallel Processing Symp., Geneva, Switzerland, 1–5 April 1997

4 YAYLA, G., KRISHNAMOORTHY, A.V., MARSDEN, G.C., and ESENER, S.C.: 'A prototype 3D optically interconnected neural network', *Proc. IEEE*, 1994, **82**, pp. 1749–1762

5 WOODWARD, T.K., KRISHNAMOORTHY, A.V., LENTINE, A.L., and CHIROVSKY, L.M.F.: 'Optical receivers for optoelectronic VLSI', *IEEE J. Sel. Top. Quantum Electron.*, 1996, **2**, pp. 106–116

6 WILLIAMS, G.: 'Lightwave receivers' *in* TINGYE LI (Ed): 'Topics in lightwave systems' (Academic Press, 1991), pp.79–148

7 WESTE, N.H.E., and ESHRAGHIAN, K.: 'Principles of CMOS VLSI design' (Addison Wesley, New York, 1993)

GaAs-based, 1.55μm high speed, high saturation power, low-temperature grown GaAs *pin* photodetector

Yi-Jen Chiu, S.Z. Zhang, S.B. Fleischer, J.E. Bowers and U.K. Mishra

A novel 1.55μm high speed (> 20GHz) and high saturation power (> 10mW) *pin* photodetector grown on a GaAs substrate is reported. By utilising low-temperature grown GaAs, the photodetectors can detect 1.55μm light with high bandwidth owing to the short carrier trapping time.

Introduction: For optical fibre communication, the wavelengths widely used are in the range of 1.3–1.6μm, which utilise Ge-, GaInAsP- or InP-based materials. AlGaAs/GaAs is a well developed material and such photodetectors have been integrated with high performance integrated circuits; however, its higher bandgap characteristics (E_g = 1.42eV, λ < 0.78μm, short wavelength absorption) restrict application to datacom communication. Recently, two groups [1, 2] showed that low-temperature grown GaAs (LT-GaAs) can absorb long wavelength light due to mid gap defects or As precipitates. Also, it was shown [3] that a sub-picosecond carrier trapping time was observed for 1.56μm light excitation. LT-GaAs material has been used to make high speed photodetectors [4, 5] with bandwidths > 350GHz demonstrated for travelling wave and MSM photodetectors at wavelengths < 0.82μm. However, high speed performance at long wavelengths has not yet been investigated. In this Letter, we demonstrate the first high speed, high saturation power 1.55μm *pin* photodetectors utilising LT-GaAs grown on GaAs substrate.

Growth and fabrication: A waveguide photodetector (WGPD) was designed and fabricated. Fig. 1 (top) shows a schematic diagram of the coupling facet of the devices. The optical waveguide was formed by a *pin* heterostructure (bottom of Fig. 1) which was grown in an MBE system. A 3μm $Al_{0.5}Ga_{0.5}As$ layer is used for the isolation of the optical waveguide from the bulk GaAs. The *n*- and *p*-type cladding layers ($Al_{0.2}Ga_{0.8}As$) were doped with Si and Be respectively. Two kinds of LT-GaAs layer (170 and 350nm thickness) are utilised as the absorption region (i-layer), where the growth temperature was 215°C with As_2/Ga equivalent beam pressure ratio of 12. The subsequent *in situ* annealing was at 590°C for 10min. Standard processing was used for device fabrication [5].

Measurement and results: An optical component analyser (HP 8703A, 0.13 ~20GHz) was used to measure the frequency response. The external light source was a 1.55μm laser diode. The generated microwave signal was collected by a 40GHz bandwidth probe.

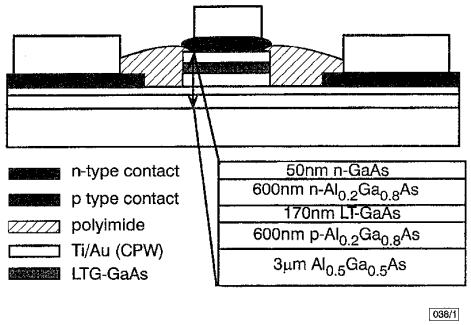

Fig. 1 *Facet view of pin photodetector*
Insert: material growth structure

Two different lengths of photodetector (denoted A and B) were fabricated. Photodetector A was 2μm wide and 35μm long (170nm thick LT-GaAs). As shown in Fig. 2, the frequency response variation is within 2dB from DC to 20GHz. Different power levels of excitation (0.75–11mW) reveal identical responses without saturation. As seen in the inset of Fig. 2, the generated microwave power shows a quadratic relation with the optical power at 20GHz, indicating that the photocurrent has a linear dependence on the optical power up to 20GHz. The measured external quantum efficiency was ~ 0.1%. The low efficiency is due to the low absorption coefficient combined with the short device length. To increase the quantum efficiency, a longer waveguide was designed. Photodetector B, with width = 2μm, length = 300μm (350nm thick LT-GaAs) was designed to improve efficiency. This device has a quantum efficiency of 1%. As seen in Fig. 3, the frequency response has ~ –4dB rolloff at 20GHz. The solid curve is the theoretical calculation which agrees quite well with the experiment. One important fact is that the response for different powers shows no nonlinear (power saturation) effects up to 20GHz.

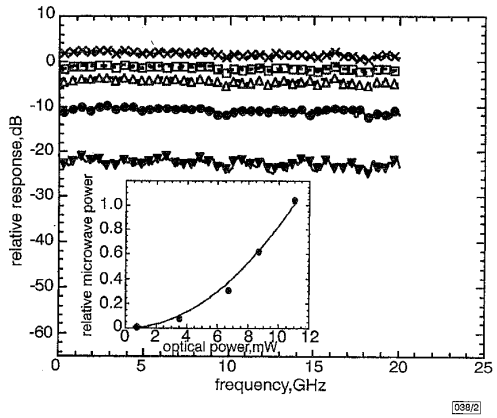

Fig. 2 *Frequency response of photodetector A (30μm long)*
——— 11mW
– –□– – 8.7mW
·····△····· 6.7mW
——●—— 3.5mW
——▼—— 750mW
Insert: photogenerated microwave power (at 20GHz) against optical power
● measurement value
——— quadratic curve fit

Analysis and discussion: For the theoretical calculation (solid curve of Fig. 3), we adopt a distributed photocurrent model. The distributed photogenerated charge is excited as light travels through the waveguide. The model includes the velocity mismatching between the optical wave and microwave, the carrier trapping time in LT-GaAs and microwave loss and boundary reflection of the input and output ends. A 300fs carrier trapping time is assumed. The response shows little dependence on the carrier trapping times for a change from 100fs to 1ps. It reveals that the factors affecting the bandwidth will not include the trapping time. The measured microwave loss has a 3.5dB drop up to 20GHz and the velocity mismatch factor ($v_{optical}/v_{microwave}$) is ~2. The loss and velocity mismatch are responsible for the limited bandwidth. A travelling wave type design would improve the performance.

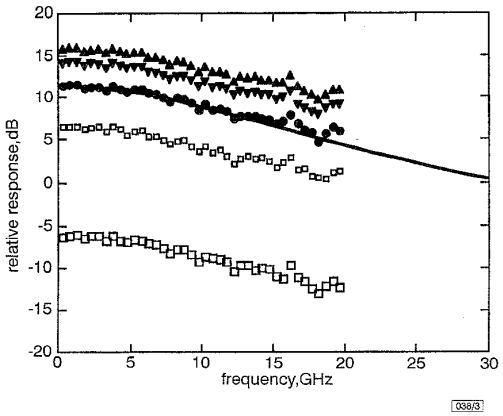

Fig. 3 *Measured and theoretical frequency response of photodetector B (300μm long) at different excitation powers*
——— theory
▲ 11mW
▼ 8.7mW
● 6.7mW
□ 3.5mW
□ 0.76mW

The low efficiency (0.1% and 1% for photodetectors A and B, respectively) is due to short carrier trapping time and low absorption coefficient. A modal absorption coefficient of ~110cm^{-1} was measured by comparing different lengths of photodetectors. The corresponding absorption length is ~ 100μm. Therefore, to achieve a high absorption, the length should be increased to several hundreds of micrometers; however, the efficiency should be at the expense of bandwidth. To improve the bandwidth-efficiency product, the growth and annealing temperature should be optimised.

Summary: We have successfully fabricated a novel LT-GaAs *pin* photodetector operating at 1.55μm. High speed and high saturation excitation power characteristics show that the LT-GaAs material has a potential for long wavelength detection in the optical fibre communication system and for integration with GaAs integrated circuits.

Acknowledgments: The authors would like to thank AFOSR/PRET and DARPA Ultrafast projects for supporting this research.

20 April 1998
Electronics Letters Online No: 19980852

Yi-Jen Chiu, S.Z. Zhang, S.B. Fleischer, J.E. Bowers and U.K. Mishra (*Electrical and Computer Engineering Department, University of California at Santa Barbara, Santa Barbara, CA 93106, USA*)

E-mail: chiu@opto.ece.ucsb.edu

References

1 SRINIVASAN, A., SADRA, K., CAMPBELL, J.C., and STREETMAN, B.G.: 'Influence of growth temperatures on the photoresponse of low temperature grown GaAs:As p-i-n diodes', *J. Electron. Mater.*, 1993, **22**, (12), pp. 1457–1459

2 WARREN, A.C., BURROUGHES, J.H., WOODALL, J.M., MCINTURFF, D.T., HODGSON, R.T., and MELLOCH, M.R.: '1.3μm p-i-n photodetector using GaAs with As precipitates (GaAs:As)', *IEEE Electron Device Lett.*, 1991, **12**, (10), pp. 527–529

3 GRENIER, P., and WHITAKER, J.F.: 'Subband gap carrier dynamics in low-temperature-grown GaAs', *Appl. Phys. Lett.*, 1997, **70**, (15), pp. 1998–2000
4 CHOU, S.Y., and LIU, M.Y.: 'Nanoscale tera-hertz metal-semiconductor-metal photodetectors', *IEEE J. Quantum Electron.*, 1992, **28**, (10), pp. 2358–2368
5 CHIU, Y.J., FLEISCHER, S.B., LASAOSA, D., and BOWERS, J.E.: 'Ultrafast (370GHz bandwidth) p-i-n traveling wave photodetector using low-temperature-grown GaAs', *Appl. Phys. Lett.*, 1997, **71**, (17), pp. 2508–2510

Linear and sensitive CMOS position-sensitive photodetector

A. Mäkynen and J. Kostamovaara

A CMOS position-sensitive photodetector (PSD) optimised for outdoor applications is presented. The PSD operates similarly to a four quadrant PSD, but instead of being fixed, its gap tracks the light spot as it moves. Test results show a significantly better performance as compared to conventional PSDs.

Introduction: Full custom CMOS technology makes it possible to implement optical detectors with good electro-optical properties and to customise their construction in order to achieve the best possible performance in a particular application [1, 2]. A linear and sensitive CMOS position-sensitive photodetector (PSD), optimised for outdoor measurements, is reported here. Outdoors PSDs are typically used to measure the angular deviation θ of a remote object with respect to the optical axis of a receiver, as depicted in Fig. 1. Typically, a lateral effect photodiode (LEP) or a four-quadrant (4Q) photodiode is used as a PSD. The 4Q PSD composed of four adjacent photodiodes has low noise and correspondingly high resolution, but as the receiver must be defocused in order to achieve the appropriate measurement field L, it tends to be very susceptible to light spot nonuniformities. Outdoors, such nonuniformities are caused by atmospheric turbulence which usually deteriorates the high resolution of the 4Q PSD. An LEP is much noisier, due to the low interelectrode resistance, but is less sensitive to atmospheric turbulence since the received beam can be accurately focused on the detector surface. Experiments have shown that outdoors the LEP provides a much better resolution than the 4Q PSD [3]. The resolution of a PSD, such as an LEP capable of using a highly focused light spot, is also less affected by the shot noise of the background illumination due to a smaller active area required to cover the same measurement field (L^2 against $4L^2$) [4]. In this Letter, we demonstrate that it is possible to combine the best properties of the LEP and the 4Q PSD, thus obtaining a high resolution and good linearity without introducing susceptibility to atmospheric turbulence, and that such a PSD can be successfully implemented using standard industrial CMOS technology.

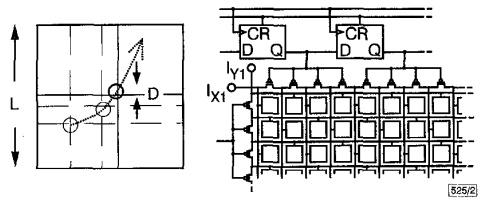

Fig. 2 *Operation principle and construction of proposed PSD*

Implementation: The operation mode of the proposed PSD is similar to that of the 4Q PSD with the exception that the position of the gap tracks the light spot electrically within the active area of the PSD (Fig. 2). The sensor is composed of a dense area array of CMOS compatible photodiodes which are alternately connected to the row and the column current lines, while these are in turn connected to two separate MOS transistor arrays which are used to divide the array into four separate areas, as depicted in Fig. 2. The high accuracy (≪μm) of the photodetector array geometry is used to establish good integral linearity, while its high resolution is based on the 'subspot' interpolation using the inherently nonlinear but highly sensitive 4Q principle. Note that a small light spot can be used due to a small gap step, which means a low turbulence sensitivity and lower background noise contribution as compared with a conventional 4Q PSD.

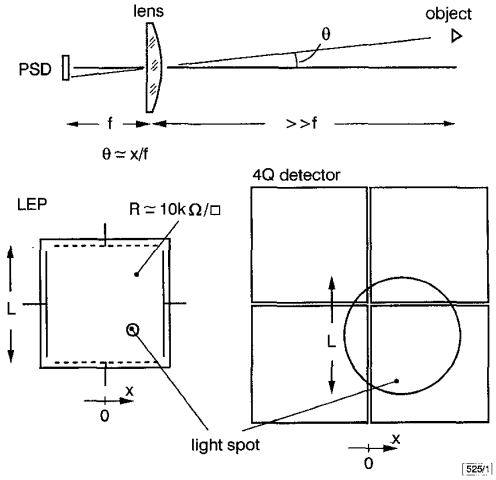

Fig. 1 *Sensing principle and PSDs used for measuring angular displacement of remote object*

The standard deviation of the lateral displacement of the measured centroid positions is

$$\sigma \simeq K/SNR \qquad (1)$$

where the scale factor K equals L and $\pi D/4$ for an LEP and the proposed PSD, respectively [4]. The signal-to-noise ratio (SNR) here is defined as the ratio between the rms-values of the total photocurrent and that of the noise current related to one quadrant or edge contact. Note that in case of an LEP, the scale factor K is determined by the extent of the measurement field, whereas in the case of the proposed PSD, the scale factor of the interpolator is roughly equal to the size of the light spot D, which in this case does not limit the extent of the measurement field and is typically much smaller than the measurement field. Thus, the resolution of the proposed PSD (standard deviation σ) compared to an LEP (σ_{LEP}), assuming equal responsivity and size of measurement field, is

$$\sigma \simeq \frac{D}{L}\frac{\pi}{4}\frac{i_n}{i_{nLEP}}\sigma_{LEP} \qquad (2)$$

where i_n and i_{nLEP} are the noises of the proposed PSD and the LEP. Since D/L and i_n/i_{nLEP}, might both typically be in the order of 0.1, the resolution of the proposed PSD could well be two orders of magnitude better than that of an LEP.

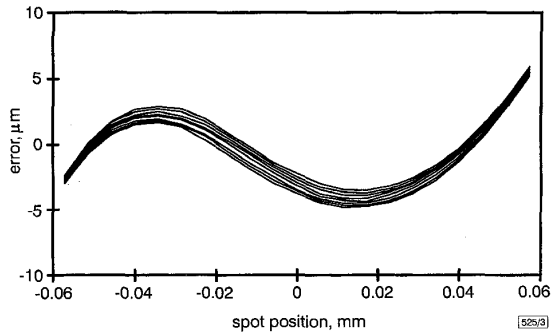

Fig. 3 *Lateral transfer characteristics of interpolator*
σ ≃ 2.7μm

The PSD was implemented using standard 1.2μm CMOS technology, and was composed of 100 × 100 well-substrate photodiodes occupying a total area of 2.5 × 2.5mm². The array pitch was 25μm and the fill factor was 68%. In the prototype, the transistor gates were driven by the logic output signals from a